



# Comparison of quantitative imaging parameters using cardiovascular magnetic resonance between cardiac amyloidosis and hypertrophic cardiomyopathy: inversion time scout versus T1 mapping

Bo Da Nam<sup>1,2</sup> · Sung Mok Kim<sup>1,3,5</sup> · Hye Na Jung<sup>1,4</sup> · Yiseul Kim<sup>1</sup> · Yeon Hyeon Choe<sup>1,3</sup>

Received: 9 January 2018 / Accepted: 26 May 2018 / Published online: 30 May 2018  
© Springer Science+Business Media B.V., part of Springer Nature 2018

## Abstract

To compare inversion time (TI) parameters, native T1, and extracellular volume (ECV) on cardiac magnetic resonance (CMR) imaging between patients with cardiac amyloidosis (CA) or hypertrophic cardiomyopathy (HCMP). Forty six patients with biopsy-confirmed CA and 30 patients with HCMP who underwent CMR were included. T1 and TI values were measured in the septum and cavity of the left ventricle on T1 mapping and TI scout images. TI values were selected at nulling point for each myocardium and blood pool. Native T1, ECV, and TI interval values were significantly different between the CA ( $1170.5 \pm 86.4$  ms,  $56.7 \pm 12.2$ ,  $-11.5 \pm 28.4$  ms) and HCMP ( $1059.5 \pm 63.4$  ms,  $28.5 \pm 5.8$ ,  $66.2 \pm 25.4$  ms) (all  $p < 0.001$ ). The diagnostic performance of the TI interval (area under the ROC curve, 0.975) was not inferior to that of the ECV (0.980,  $p = 0.776$ ), and it was superior to that of the native T1 (0.845,  $p = 0.004$ ). The diagnostic performance of TI interval was comparable to that of ECV for differential diagnosis between CA and HCMP. TI interval showed the feasibility as quantitative CMR parameter when T1 mapping images are not available.

**Keywords** Amyloidosis · Cardiovascular magnetic resonance · Extracellular volume · Hypertrophic cardiomyopathy · Inversion time

## Abbreviations

AUC	Area under the ROC curve
CA	Cardiac amyloidosis
CMR	Cardiovascular magnetic resonance
ECV	Extracellular volume

GRAPPA	Generalized auto-calibrating partially parallel acquisitions
HCMP	Hypertrophic cardiomyopathy
LGE	Late gadolinium enhancement
LV	Left ventricle
LVEDV	Left ventricular end-diastolic volume
LVESV	Left ventricular end-systolic volume
MOLLI	Modified look-locker inversion recovery
TR	Repetition time
TE	Echo time
ROC	Receiver-operating characteristic
SA	Short-axis
SSFP	Steady-state free precession
SV	Stroke volume
TI	Inversion time

✉ Sung Mok Kim  
sungmok\_kim@hanmail.net

<sup>1</sup> Department of Radiology, Samsung Medical Center, Sungkyunkwan University School of Medicine, Seoul, Republic of Korea

<sup>2</sup> Present Address: Department of Radiology, Soonchunhyang University Seoul Hospital, Soonchunhyang University College of Medicine, Seoul, Republic of Korea

<sup>3</sup> Cardiovascular Imaging Center, Heart Vascular and Stroke Institute, Samsung Medical Center, Seoul, Republic of Korea

<sup>4</sup> Present Address: Department of Radiology, Korea University Guro Hospital, Korea University College of Medicine, Seoul, Republic of Korea

<sup>5</sup> Department of Radiology and Cardiovascular Imaging Center, Cardiac and Vascular Center, Samsung Medical Center, Sungkyunkwan University School of Medicine, 81 Ilwon-ro, Gangnam-gu, Seoul 06351, Republic of Korea

## Introduction

Cardiac amyloidosis (CA) has a poor prognosis [1], so diagnosis for treatment decisions is important. Although endomyocardial biopsy is the most accurate method for the diagnosis of CA, the procedure has risks due to its invasiveness

[2]. Echocardiography is the most commonly used non-invasive imaging method, but it is insensitive in the early stage of CA [3]. Several studies have shown that CA can be diagnosed using cardiovascular magnetic resonance (CMR) with late gadolinium enhancement (LGE) images because of its characteristic enhancement pattern, including diffuse, global subendocardial enhancement [4–6], but CA might show atypical features, such as patchy or focal enhancement [7]. The most common LGE patterns of hypertrophic cardiomyopathy (HCM) are patchy and multifocal distributions [8–10], so differentiating between CA and HCM can be difficult if the CA does not show specific LGE patterns. In addition, amyloid deposition shortens the T1 time of the myocardium, making it difficult to identify the appropriate nulling time during acquisition of the LGE images [4].

T1 mapping and extracellular volume (ECV) have been introduced as quantitative parameters according to the development of the CMR techniques [11, 12]. Recently, studies have compared patients with CA, HCM, or non-amyloid cardiomyopathy using values of native T1 mapping and ECV [13–15]. However, additional acquisition time is required to obtain T1 mapping, and acquiring T1 mapping images both before and after injection of gadolinium contrast is required to calculate ECV. The inversion time (TI) scout images, which are a type of routine image, generally are used to obtain LGE images corresponding to the optimal nulling time. From the TI scout images, we can determine the nulling time of the LV cavity and myocardium. Indeed, assessment of the temporal order of nulling on the TI scout images in patients with CA has been used to establish the characteristics of CA [16]. We hypothesized that quantitative parameters obtained from the TI scout images will demonstrate characteristic values for CA patients. Thus, the purpose of this study was to compare the native T1, ECV, and TI parameters on CMR imaging between patients with CA or HCM and to evaluate whether the TI parameter can replace the ECV as a quantitative CMR parameter.

## Methods

### Patient population

Between October 2011 and April 2016, 46 consecutive patients with histopathologically diagnosed CA of the light-chain type were included in this study. All patients underwent CMR examination at the time of pathologic diagnosis. The mean interval between pathologic diagnosis and CMR study was  $2.7 \pm 2.4$  days (median 2 days; range 0–10 days). In addition, 30 consecutive patients with clinically diagnosed HCM of a concentric or septal type and ten asymptomatic subjects who underwent screening CMR for a health checkup at the Health Promotion Center of our institute

were included in this study. None of ten control subjects had hypertension or diabetes. This study was approved by the Institutional Review Board at Samsung Medical Center, one of the major tertiary referral centers in Seoul, Korea, and the requirement for informed consent for the use of patient data was waived.

### CMR imaging protocol

All patients underwent cardiac MRI with a 1.5 T scanner (Magnetom Avanto, Syngo MR B17 version; Siemens Healthcare, Erlangen, Germany) and a 32-channel phased-array receiver coil during repeated breath-holds. CMR scans consisted of localizing images (axial, coronal, and sagittal), cine scans, native T1 mapping, late gadolinium enhancement scans, and post-T1 mapping.

After localization, cine images of the left ventricle (LV) were acquired using a steady-state free precession (SSFP) sequence on 4-, 3-, and 2-chambers and short-axis (SA) views for obtaining 30 contiguous SA slices to include the entire LV with a 6-mm slice thickness and 4-mm intersection gaps. Balanced SSFP cine images with the generalized auto-calibrating partially parallel acquisitions (GRAPPA; Siemens Medical Solutions, Erlangen, Germany) reconstruction algorithm were obtained during multiple breath-holds. Cine images were acquired with the following parameters: repetition time/echo time, 3.31 ms/1.31 ms; flip angle  $72^\circ$ ; phases per cardiac cycle 30; field of view  $240 \times 300$  mm<sup>2</sup>; matrix  $256 \times 150$ ; and generalized auto-calibrating partially parallel acquisitions (GRAPPA) acceleration factor, 2.

T1 mapping images were acquired with modified Look-Locker inversion-recovery (MOLLI) sequence. The pre-contrast MOLLI was composed of 5 images over 5 heartbeats after the first inversion pulse and 3 images over 3 heartbeats after the second inversion pulse [a 5(3)-3 protocol with a pause of 3 heartbeats]. Finally, eight images during 11 heartbeats were obtained, and T1 maps were generated after registration of individual inversion images with inline motion correction prior to non-linear curve fitting using the 3-parameter signal model. The post-contrast MOLLI scheme was 4(1)-3(1)-2 over 11 heartbeats with three inversion pulses. Finally, nine images with different TIs were acquired. The following scan parameters were used: slice thickness 8 mm; flip angle  $35^\circ$ ; field of view  $360$  mm  $\times$   $307$  mm; initial TI 120 ms; TI increment 80 ms; voxel size  $1.87 \times 1.88 \times 8$  mm<sup>3</sup>; TR (Repetition time)/TE (Echo time), 2.4/1.01 ms; partial Fourier, 7/8; and GRAPPA parallel imaging factor, 2. Post-contrast images were acquired at the same positions as the pre-contrast images within 15 min after the injection. All scans were carried out by qualified technicians and supervised by an experienced radiologist.

The TI scout gradient echo sequence had the following parameters: 8 mm thick, mid ventricle level, TR 23.58 ms, TE 1.11 ms, flip angle 30°, generated using 20 or 30 ms increments (depending on heart rate) from 85 to 795 ms.

### Anatomical and functional analysis of the left ventricle

CMR image analyses were performed by one experienced investigator (Y.K) blinded to the clinical results. Septal and posterior wall thicknesses were measured on SA images at the LV mid-ventricular level. Quantitative evaluation of LV volume and mass at end diastole and end systole was performed. Frames with the largest and smallest ventricular volumes were chosen as end diastole and end systole, respectively. The LV end-diastolic volume (LVEDV), LV end-systolic volume (LVESV), LV ejection fraction, stroke volume (SV), cardiac output, and LV mass were calculated from the SA cine images using ARGUS™ software (Siemens Healthcare, Erlangen, Germany) with semiautomatic contour detection. Manual correction of the automatically rendered endo- and epicardial contours was performed in all data-sets, and the papillary muscles and myocardial trabeculations were included in the ventricular cavity. The LV mass was measured by multiplying the sum of total LV myocardial volume from the cine images by specific gravity of the myocardium.

### Analysis of T1 mapping with ECV quantification and TI scout

For the acquisition of myocardial T1 values, ROIs for signal intensity were drawn manually in the septum of the pre- and post-contrast T1 maps at the mid-ventricular level. The T1 value of blood was measured by positioning a circular ROI in the LV cavity while avoiding the papillary muscle. The ECV of the myocardium was calculated as follows:  $ECV (\%) = (\Delta R1_m / \Delta R1_b) \times (1 - \text{hematocrit level}) \times 100$ , where R1 is  $1/T1$ ;  $R1_m$  is the R1 of the myocardium;  $R1_b$  is the R1 of the blood; and  $\Delta R1$  is the change in relaxivity. The change in relaxivity ( $\Delta R1$ ) was determined with the following equation:  $\Delta R1 = R1_{\text{post}} - R1_{\text{pre}}$ , where  $R1_{\text{post}}$  and  $R1_{\text{pre}}$  are the R1 after and before contrast administration, respectively [17, 18].

The TI scout used for delayed hyper-enhancement was the time to complete nulling of the signal of the myocardium. TI scout images were acquired at 10 min after contrast injection. The temporal order of nulling of the contrasted blood pool in the LV cavity and myocardium (interventricular septum) was recorded in each case from the TI scout sequence. We compared the TI of the nulling point between the CA, HCMP, and control groups. We also analyzed the intervals of TI obtained

from the LV cavity and myocardial septum in those groups (Fig. 1).

### Statistical analysis

Statistical analysis was performed with SAS version 9.4 (SAS Institute, Cary, NC) and R 3.4.0 (Vienna, Austria). The clinical features and CMR parameters between the CA, HCMP, and control groups were compared using Fisher's exact test for categorical variables and Kruskal–Wallis test for continuous variables. Comparisons of TI between the CA, HCMP, and control groups were performed by ANOVA and Kruskal–Wallis tests; for the post-hoc analysis, we used Mann–Whitney U test with Bonferroni correction. Receiver-operating characteristic (ROC) curve analysis was used to test the predictive performance of TI and intervals of TI between the LV cavity and myocardium and the results were presented as the area under the ROC curve (AUC) and 95% confidence interval (CI). The comparison of AUC for diagnostic performance among CMR parameters was analyzed by using the DeLong method [19]. The correlation between the representative parameter, such as ECV and other CMR parameters, was calculated with Spearman's correlation coefficient. Interobserver agreement for the measurement of TI scout and T1 mapping was analyzed with intraclass correlation coefficients (ICCs). ICC values of 0.20 or less were indicative of poor agreement; 0.21–0.40 was considered fair; 0.41–0.60, moderate; 0.61–0.80, good; and 0.81 or more, excellent correlation. In all statistical analyses,  $p$  values  $< 0.05$  were considered statistically significant.

## Results

### Patient characteristics

Patient characteristics for all groups are summarized in Table 1. There were no significant differences in age or sex among the CA, HCMP, and control groups. Body surface area was about 0.1 m<sup>2</sup> higher in patients with HCMP than in other groups ( $p < 0.001$ ). Patients with CA had 5–6% significantly lower hematocrit level than did patients with HCMP ( $p < 0.001$ ). Among the CMR parameters, left ventricular mass index was lower in patients with CA than patients with HCMP by 30 g/m<sup>2</sup> ( $p < 0.001$ ). There was a significant difference between patients with CA and HCMP in LVEF, LVEDV and SV among the remaining CMR parameters (all  $p < 0.001$ ).

### TI of the nulling point and TI interval obtained from the myocardium and LV cavity in CA, HCMP, and control groups

There were significant differences in TI in the myocardial septum among the CA, HCMP, and control groups

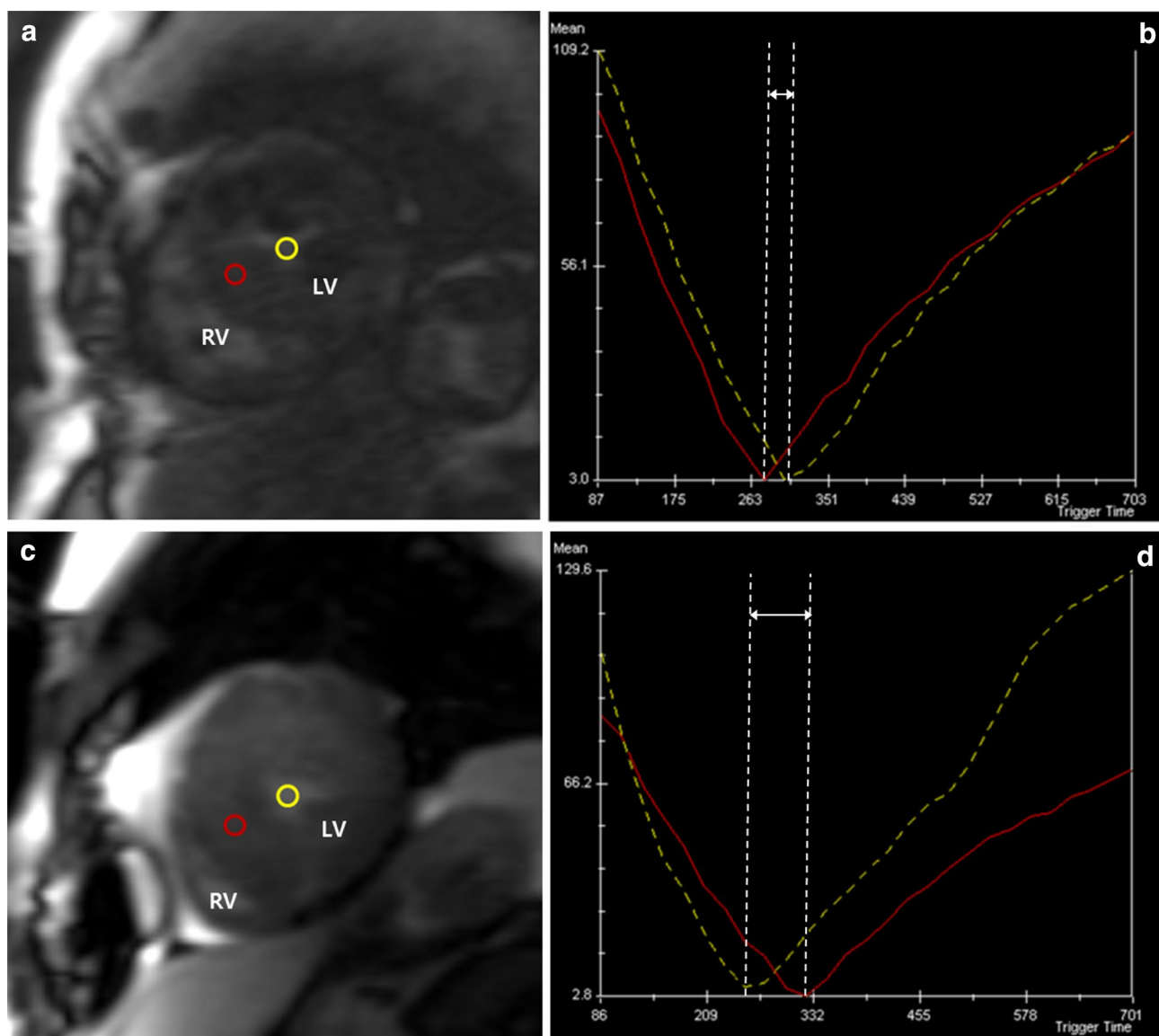


**Fig. 1** TI scout images and TI curve in patients with cardiac amyloidosis and hypertrophic cardiomyopathy. Inversion time (TI) scout images with ROI measurement of LV cavity (yellow circle) and myocardium (red circle) and TI curve in patients with cardiac amyloidosis and hypertrophic cardiomyopathy. **a** and **b** TI interval (TI value

of the myocardial septum—TI value of the left ventricular cavity, arrow in **b**),  $-22$  ms in a 52-year-old man with cardiac amyloidosis. **c** and **d** TI interval (arrow in **d**),  $70$  ms in a 58-year-old man with hypertrophic cardiomyopathy. [LV left ventricle, RV right ventricle on short-axis views (**a**, **c**)]

(Fig. 2a). Patients with CA had significantly decreased TI of the myocardium ( $192.1 \pm 33.2$  ms) compared to patients with HCMP ( $234.6 \pm 29.0$  ms,  $p < 0.001$ ) and controls ( $244.6 \pm 19.8$  ms,  $p < 0.001$ ). The TI of the LV cavity was increased in patients with CA ( $203.5 \pm 36.9$  ms) compared to patients with HCMP ( $168.4 \pm 35.7$  ms,  $p < 0.001$ ) and controls ( $160.7 \pm 18.1$  ms,  $p < 0.001$ ) (Fig. 2b). There were no statistically significant differences in the TI of the myocardium or the TI of the LV cavity between HCMP patients and controls ( $p = 0.320$  and  $0.937$ , respectively) (Table 2).

The TI interval differed significantly between the myocardium and the LV cavity (Fig. 3). The CA group had a decreased TI interval ( $-11.5 \pm 28.4$  ms,  $p < 0.001$ ) compared to the HCMP group ( $66.2 \pm 25.4$  ms). The TI interval differed significantly between the CA and control groups ( $83.9 \pm 16.8$  ms,  $p < 0.001$ ), but not between the HCMP and control group ( $p = 0.096$ ).

**Table 1** Basic characteristics of CA, HCMP, and control groups

	CA (n=46)	HCMP (n=30)	P value <sup>†</sup>	Control (n=10)	P value <sup>‡</sup>
Age (years) (range)	59.2±9.3	56.9±11.4	0.324	53.3±6.6	0.196
Sex (M:F)	30:16	26:4	0.038	5:5	0.040
BSA* (m <sup>2</sup> )	1.7±0.2	1.8±0.2	<0.001	1.7±0.1	0.001
Hct* (%)	38.7±4.5	44.4±3.9	<0.001	44.1±4.0	<0.001
CMR parameter					
LVEF* (%)	57.3±13.1	69.2±7.5	<0.001	66.1±4.1	<0.001
LVEDV* (ml)	112.4±34.5	139.4±32.4	0.001	118.8±20.7	0.004
LVESV (ml)	48.9±27.1	43.7±18.7	0.541	45.2±18.5	0.834
SV* (ml)	63.5±20.4	95.7±21.7	<0.001	78.0±10.3	<0.001
CO* (l/min)	4.8±1.3	6.1±1.4	<0.001	5.2±0.6	<0.001
LVM* (g)	169.0±55.2	246.5±62.6	<0.001	94.2±25.7	<0.001
LVEDVi* (ml/m <sup>2</sup> )	67.2±20.0	75.7±16.6	0.009	69.1±11.1	0.028
LVESVi (ml/m <sup>2</sup> )	29.4±17.0	23.9±11.4	0.059	26.0±9.5	0.155
SVi* (ml/m <sup>2</sup> )	37.8±10.8	51.8±9.4	<0.001	45.4±5.0	<0.001
LVMi* (g/m <sup>2</sup> )	100.3±27.1	133.9±31.2	<0.001	54.2±11.7	<0.001

CA cardiac amyloidosis, HCMP hypertrophic cardiomyopathy, BSA body surface area, Hct hematocrit, CMR cardiovascular magnetic resonance, LVEF left ventricular ejection fraction, LVEDV left ventricular end-diastolic volume, LVESV left ventricular end-systolic volume, SV stroke volume, CO cardiac output, LVM left ventricular mass, i index, myo myocardium, LV left ventricle

\*Statistically significant results of the difference between the findings of CA, HCMP and control groups (p<0.05)

<sup>†</sup>P value between groups of CA and HCMP

<sup>‡</sup>P value between groups of CA and control

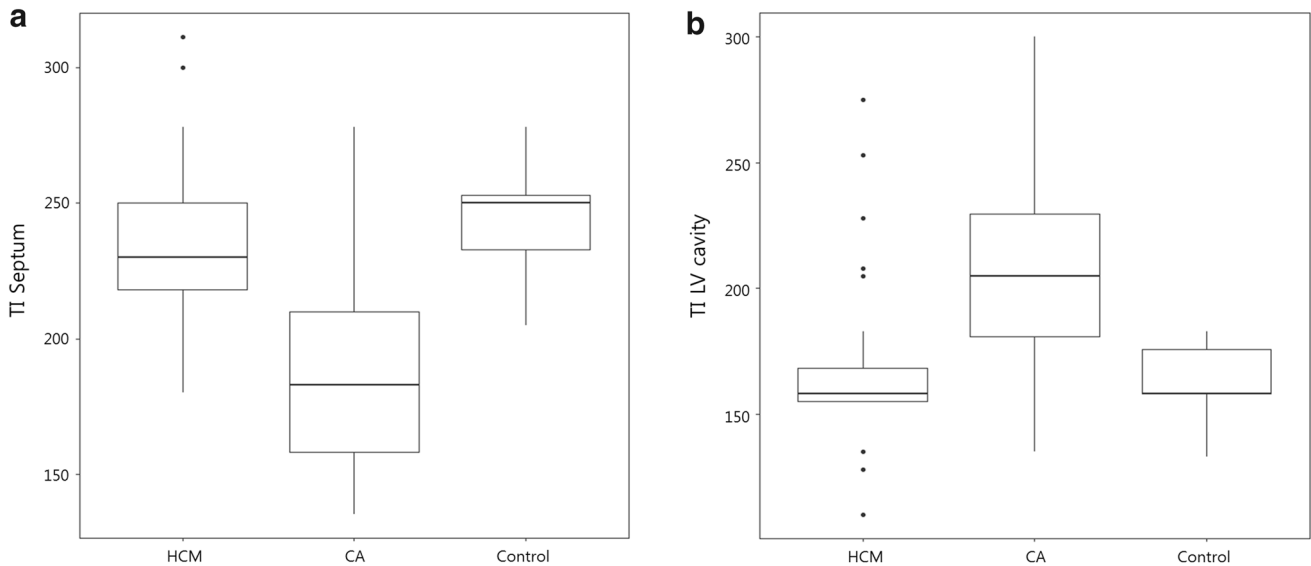


**Fig. 2** T1 values in hypertrophic cardiomyopathy, cardiac amyloidosis, and healthy controls. Inversion time (TI) values obtained from the TI scout of the **a** myocardial septum and **b** left ventricular cavity in three groups of patients. Comparisons between subgroups: **a**

Hypertrophic cardiomyopathy (HCMP) versus cardiac amyloidosis (CA),  $p<0.001$ ; CA versus control,  $p<0.001$ ; HCMP versus control,  $p=0.320$ . **b** HCMP versus CA,  $p<0.001$ ; CA versus control,  $p=0.001$ ; HCMP versus control,  $p=0.937$

**Native T1 mapping and ECV in CA, HCMP, and control groups**

Native T1 mapping differed significantly between the CA (1170.5±86.4 ms), HCMP (1059.5±63.4 ms), and

control groups (965.0±49.9 ms,  $p<0.001$ ). Posthoc analyses also revealed significant differences between the CA and HCMP groups, CA and control groups, and HCMP and control groups (all  $p<0.001$ ) (Fig. 4a). Patients with CA showed increased ECV values (56.7±12.2) compared



**Table 2** Comparison with CMR parameters between CA, HCMP, and control groups

	CA (n=46)	HCMP (n=30)	P value <sup>†</sup>	Control (n=10)	P value <sup>‡</sup>
Native T1* (myo) (ms)	1170.5 ± 86.4	1059.5 ± 63.4	< 0.001	965.0 ± 49.9	< 0.001
ECV* (%)	56.7 ± 12.2	28.5 ± 5.8	< 0.001	24.8 ± 4.7	< 0.001
TI* (myo)	192.1 ± 33.2	234.6 ± 29.0	< 0.001	244.6 ± 19.8	< 0.001
TI* (LV cavity)	203.5 ± 36.9	168.4 ± 35.7	< 0.001	160.7 ± 18.1	< 0.001
TI interval* (myo-LV)	- 11.5 ± 28.4	66.2 ± 25.4	< 0.001	83.9 ± 16.8	< 0.001

CMR cardiovascular magnetic resonance, CA cardiac amyloidosis, HCMP hypertrophic cardiomyopathy, ECV extracellular volume, TI inversion time, myo myocardium, LV left ventricle

\*Statistically significant results of the difference between the findings of CA, HCMP and control groups ( $p < 0.05$ )

<sup>†</sup>P value between groups of CA and HCMP

<sup>‡</sup>P value between groups of CA and control

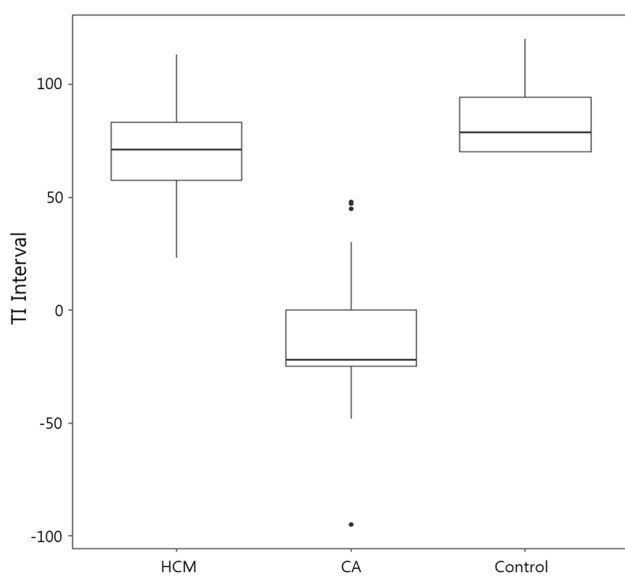


**Fig. 3** TI interval in hypertrophic cardiomyopathy, cardiac amyloidosis, and healthy controls. Inversion time (TI) intervals (TI value of the myocardial septum—TI value of the left ventricular cavity) in three groups of patients. Comparisons between subgroups: Hypertrophic cardiomyopathy (HCMP) versus cardiac amyloidosis (CA),  $p < 0.001$ ; CA versus control,  $p < 0.001$ ; HCMP versus control,  $p = 0.096$

to patients with HCMP ( $28.5 \pm 5.8$ ,  $p < 0.001$ ) and controls ( $24.8 \pm 4.7$ ,  $p < 0.001$ ) (Fig. 4b). The ECV differed significantly between the HCMP and control groups ( $p = 0.016$ ).

Interobserver reliability was excellent for the measurement of TI scout and native T1 mapping [ICCs for TI scout, 0.936 (CI 0.866–0.970); for native T1 mapping, 0.898 (CI 0.786–0.952)].

### Comparison of TI values, native T1 Mapping and ECV for differential diagnosis between HCMP and CA

In the comparison of diagnostic performance of the TI interval (myocardium-LV cavity), native T1 mapping, and ECV between HCMP and CA, ROC curve analysis (Fig. 5) showed an AUC of 0.975 for the TI interval, which was not significantly different from that of the ECV (0.980,  $p = 0.776$ ). The AUC for the TI interval was significantly greater than that for native T1 mapping (0.845,  $p = 0.004$ ). The optimal cutoff values obtained from Youdens index were 25 for the TI interval, 1130.9 for the native T1 value, and 40.1 for the ECV. Each sensitivity and specificity is as follows: TI interval, 0.967, 0.891; native T1, 0.761, 0.833; ECV, 0.957, 0.933.

Spearman rank correlations were performed to identify which CMR parameters, such as TI value and LV mass index, were correlated with ECV. There was a strong correlation between ECV and TI interval ( $r = -0.724$ ,  $p < 0.001$ ) and a moderate correlation between the TI of the myocardium and ECV ( $r = -0.581$ ,  $p < 0.001$ ) (Table 3).

## Discussion

The main finding of our study was that the TI interval between the myocardium and LV cavity showed a higher AUC value (0.975) than did the native T1 (0.845,  $p = 0.004$ ) and showed non-inferiority to the ECV (0.980,  $p = 0.776$ ) for differential diagnosis between CA and HCMP. In the correlation analysis of CMR parameters and ECV, the TI interval showed the strongest correlation with ECV ( $r = -0.724$ ,  $p < 0.001$ ).

Pandey et al. [16] reported diagnostic utility for the presence of myocardial amyloidosis using the pattern of nulling on the TI scout sequence of CMR and analyzed the TI scout sequence with specific attention to the order of temporal nulling between the myocardium, blood

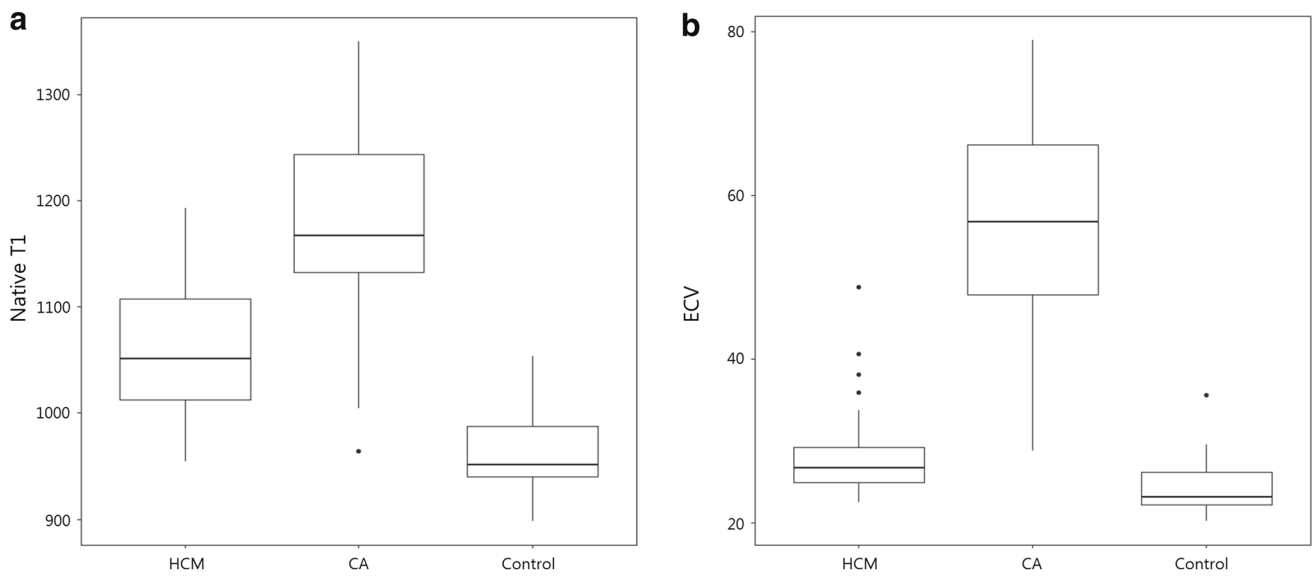


**Fig. 4** Native T1 (a) and ECV (b) in hypertrophic cardiomyopathy, cardiac amyloidosis, and healthy controls. Comparisons between subgroups: **a** Hypertrophic cardiomyopathy (HCMP) versus cardiac amy-

loidosis (CA),  $p < 0.001$ ; CA versus control,  $p < 0.001$ ; HCMP versus control,  $p < 0.001$ . **b** HCMP versus CA,  $p < 0.001$ ; CA versus control,  $p < 0.001$ ; HCMP versus control,  $p = 0.016$ . ECV extracellular volume

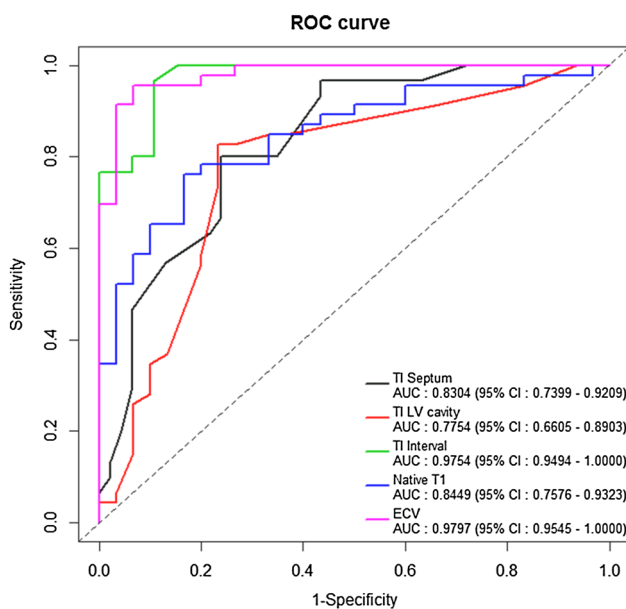


**Fig. 5** ROC curve for native T1, ECV, and TI interval. Receiver-operating characteristic (ROC) curves to detect the diagnostic performance of native T1, extracellular volume (ECV) and inversion time (TI) interval for differential diagnosis between cardiac amyloidosis and hypertrophic cardiomyopathy. AUC area under the curve

pool, and spleen. They found that patients with myocardial amyloid infiltration null the myocardium before the blood pool, while non-amyloid patients null the blood pool before the myocardium. On the basis of their findings, we explored a new CMR parameter using TI scout and T1 mapping images. We found two distinctive results:

**Table 3** Correlation of CMR parameters and ECV

ECV vs.	Case n	Rho	P value
TI interval	86	- 0.705	< 0.001
TI (myo)	86	- 0.597	< 0.001
TI (LV cavity)	86	0.323	0.003
LVMI	86	0.205	0.063

A correlation adjusting for sex, BSA and Hct was performed

CMR cardiovascular magnetic resonance, ECV extracellular volume, TI inversion time, myo myocardium, LV left ventricle, LVMI LVmass index

(1) Patients with CA had significantly decreased TI of the myocardium ( $192.1 \pm 33.2$  ms) compared to patients with HCMP ( $234.6 \pm 29.0$  ms,  $p < 0.001$ ). This finding can be explained by shortening of the TI caused by higher ECV in CA patients than HCMP patients. Previous investigators [12, 13, 15] have also found that patients with CA have significantly higher ECV than patients with HCMP. (2) Patients with CA showed increased TI in the LV cavity ( $203.5 \pm 36.9$  ms), compared to patients with HCMP ( $168.4 \pm 35.7$  ms,  $p < 0.001$ ) or healthy controls ( $160.7 \pm 18.1$  ms,  $p = 0.001$ ). The pathophysiology of this phenomenon is not well understood, but Maceira et al. [20] reported that blood gadolinium clearance is significantly faster in amyloid patients, resulting in a higher blood T1 over time and a lower T1 of the myocardium compared to controls. These opposing effects result in a markedly smaller difference in TI between the blood and myocardium in the amyloid patients compared to healthy controls.

It can be assumed that an increased amyloid load affects renal function, resulting in disturbance of gadolinium clearance.

To our knowledge, this is the first study to report an increased TI of the blood pool in patients with CA compared to healthy controls and HCMP patients. We speculated that the TI interval between the myocardium and LV cavity would differ significantly between patients with CA and HCMP. Indeed, we revealed a remarkable difference in TI interval between patients with CA ( $-11.5 \pm 28.4$  ms) and those with HCMP ( $66.2 \pm 25.4$  ms,  $p < 0.001$ ). Thus, the TI interval might have potential as a method for diagnosing cardiac involvement of amyloidosis and differential diagnosis for HCMP. In our study, we reported an AUC of 0.975, which represents the diagnostic performance of the TI interval between the myocardium and LV cavity. This AUC value, was similar to other CMR parameters, such as ECV, which have been highly useful in the diagnosis of cardiac amyloidosis (AUC, 0.980,  $p = 0.776$ ), and superior to the native T1 (AUC, 0.845,  $p = 0.004$ ).

Several previous studies of CMR have investigated non-invasive techniques for the diagnosis of myocardial amyloidosis, and the usefulness of CMR has been noted [13–16, 21–24]. Previous investigators [13, 14] found that T1 mapping can differentiate patients with cardiac involvement of amyloidosis from normal controls with high diagnostic accuracy and from patients with hypertrophic cardiomyopathy or aortic stenosis, two other conditions causing LV hypertrophy. It is well known that cardiac involvement in amyloidosis leads to excessive accumulation of extracellular contrast agents and a subsequent marked increase in ECV [15, 21, 23]. The ECV is considered to be a more accurate and reliable parameter than the native T1 [12, 21, 22]. We found a strong correlation between the diagnostic performance of ECV and TI interval in a Spearman rank correlation test. Thus, the TI interval may be considered as another potential parameter, especially when T1 mapping is not available. However, since the number of patients in our study was relatively small, the clinical application of this parameter should be verified in larger cohort studies.

Our study had several limitations, mainly its single-center, retrospective study design. These aspects of our study design limit the generalizability of the findings and raise the possibility of selection bias. In addition, the sample size was relatively small. However, we tried to include all patients with histopathologically proven CA by endocardial biopsy. Second, we analyzed multiple CMR parameters at the interventricular septum and interpreted these as representative of the whole myocardium. Third, a comparison with echocardiography was not performed because it was outside the scope of the study.

## Conclusions

The diagnostic performance of the TI interval between the myocardium and LV cavity was superior to that of the native T1 and non-inferior to that of the ECV for differential diagnosis between CA and HCMP. In addition, the TI interval showed a strong correlation with ECV. We suggest that the TI interval has the potential to replace ECV as a quantitative CMR parameter when T1 mapping images are not available.

**Author contributions** SMK was the guarantor of the entire study. BDN, SMK contributed to the conception, design and, acquisition of data, analysis and interpretation of data, and drafting of the paper. HNJ contributed to the study collection, analysis and interpretation of data, and drafting of the paper. YK contributed to the acquisition of data, analysis and interpretation of data. YHC contributed to the analysis and interpretation of data, and drafting of the paper.

## Compliance with ethical standards

**Conflict of interest** The authors declared that they have no conflict of interest.

## References

- Kyle RA, Greipp PR, O'Fallon WM (1986) Primary systemic amyloidosis: multivariate analysis for prognostic factors in 168 cases. *Blood* 68(1):220–224
- Cooper LT, Baughman KL, Feldman AM, Frustaci A, Jessup M, Kuhl U, Levine GN, Narula J, Starling RC, Towbin J, Virmani R (2007) The role of endomyocardial biopsy in the management of cardiovascular disease: a scientific statement from the American Heart Association, the American College of Cardiology, and the European Society of Cardiology. Endorsed by the Heart Failure Society of America and the Heart Failure Association of the European Society of Cardiology. *J Am Coll Cardiol* 50(19):1914–1931
- Kwong RY, Falk RH (2005) Cardiovascular magnetic resonance in cardiac amyloidosis. *Circulation* 111(2):122–124
- vanden Driesen RI, Slaughter RE, Strugnell WE (2006) MR findings in cardiac amyloidosis. *AJR Am J Roentgenol* 186(6):1682–1685
- Vogelsberg H, Mahrholdt H, Deluigi CC, Yilmaz A, Kispert EM, Greulich S, Klingel K, Kandolf R, Sechtem U (2008) Cardiovascular magnetic resonance in clinically suspected cardiac amyloidosis: noninvasive imaging compared to endomyocardial biopsy. *J Am Coll Cardiol* 51(10):1022–1030
- Wagner A, Mahrholdt H, Holly TA, Elliott MD, Regenfus M, Parker M, Klocke FJ, Bonow RO, Kim RJ, Judd RM (2003) Contrast-enhanced MRI and routine single photon emission computed tomography (SPECT) perfusion imaging for detection of subendocardial myocardial infarcts: an imaging study. *Lancet* 361(9355):374–379
- Syed IS, Glockner JF, Feng D, Araoz PA, Martinez MW, Edwards WD, Gertz MA, Dispenzieri A, Oh JK, Bellavia D, Tajik AJ, Grogan M (2010) Role of cardiac magnetic resonance imaging in the detection of cardiac amyloidosis. *JACC Cardiovasc Imaging* 3(2):155–164
- Mahrholdt H, Wagner A, Judd RM, Sechtem U, Kim RJ (2005) Delayed enhancement cardiovascular magnetic resonance



- assessment of non-ischaemic cardiomyopathies. *Eur Heart J* 26(15):1461–1474
9. Moon JC, McKenna WJ, McCrohon JA, Elliott PM, Smith GC, Pennell DJ (2003) Toward clinical risk assessment in hypertrophic cardiomyopathy with gadolinium cardiovascular magnetic resonance. *J Am Coll Cardiol* 41(9):1561–1567
  10. Wilson JM, Villareal RP, Hariharan R, Massumi A, Muthupillai R, Flamm SD (2002) Magnetic resonance imaging of myocardial fibrosis in hypertrophic cardiomyopathy. *Tex Heart Inst J* 29(3):176–180
  11. Wong TC (2014) Cardiovascular magnetic resonance imaging of myocardial interstitial expansion in hypertrophic cardiomyopathy. *Curr Cardiovasc Imaging Rep* 7(5):9267
  12. Perea RJ, Ortiz-Perez JT, Sole M, Cibeira MT, de Caralt TM, Prat-Gonzalez S, Bosch X, Berrueto A, Sanchez M, Blade J (2015) T1 mapping: characterisation of myocardial interstitial space. *Insights Imaging* 6(2):189–202
  13. Fontana M, Banyersad SM, Treibel TA, Maestrini V, Sado DM, White SK, Pica S, Castelletti S, Piechnik SK, Robson MD, Gilbertson JA, Rowczenio D, Hutt DF, Lachmann HJ, Wechalekar AD, Whelan CJ, Gillmore JD, Hawkins PN, Moon JC (2014) Native T1 mapping in transthyretin amyloidosis. *JACC Cardiovasc Imaging* 7(2):157–165
  14. Karamitsos TD, Piechnik SK, Banyersad SM, Fontana M, Ntusi NB, Ferreira VM, Whelan CJ, Myerson SG, Robson MD, Hawkins PN, Neubauer S, Moon JC (2013) Noncontrast T1 mapping for the diagnosis of cardiac amyloidosis. *JACC Cardiovasc Imaging* 6(4):488–497
  15. Mongeon FP, Jerosch-Herold M, Coelho-Filho OR, Blankstein R, Falk RH, Kwong RY (2012) Quantification of extracellular matrix expansion by CMR in infiltrative heart disease. *JACC Cardiovasc Imaging* 5(9):897–907
  16. Pandey T, Jambhekar K, Shaikh R, Lensing S, Viswamitra S (2013) Utility of the inversion scout sequence (TI scout) in diagnosing myocardial amyloid infiltration. *Int J Cardiovasc Imaging* 29(1):103–112
  17. Diesbourg LD, Prato FS, Wisenberg G, Drost DJ, Marshall TP, Carroll SE, O'Neill B (1992) Quantification of myocardial blood flow and extracellular volumes using a bolus injection of Gd-DTPA: kinetic modeling in canine ischemic disease. *Magn Reson Med* 23(2):239–253
  18. Arheden H, Saeed M, Higgins CB, Gao DW, Bremerich J, Wyttenbach R, Dae MW, Wendland MF (1999) Measurement of the distribution volume of gadopentetate dimeglumine at echo-planar MR imaging to quantify myocardial infarction: comparison with <sup>99m</sup>Tc-DTPA autoradiography in rats. *Radiology* 211(3):698–708
  19. DeLong ER, DeLong DM, Clarke-Pearson DL (1988) Comparing the areas under two or more correlated receiver operating characteristic curves: a nonparametric approach. *Biometrics* 44(3):837–845
  20. Maceira AM, Joshi J, Prasad SK, Moon JC, Perugini E, Harding I, Sheppard MN, Poole-Wilson PA, Hawkins PN, Pennell DJ (2005) Cardiovascular magnetic resonance in cardiac amyloidosis. *Circulation* 111(2):186–193
  21. Banyersad SM, Sado DM, Flett AS, Gibbs SD, Pinney JH, Maestrini V, Cox AT, Fontana M, Whelan CJ, Wechalekar AD, Hawkins PN, Moon JC (2013) Quantification of myocardial extracellular volume fraction in systemic AL amyloidosis: an equilibrium contrast cardiovascular magnetic resonance study. *Circ Cardiovasc Imaging* 6(1):34–39
  22. Moon JC, Messroghli DR, Kellman P, Piechnik SK, Robson MD, Ugander M, Gatehouse PD, Arai AE, Friedrich MG, Neubauer S, Schulz-Menger J, Schelbert EB (2013) Myocardial T1 mapping and extracellular volume quantification: a Society for Cardiovascular Magnetic Resonance (SCMR) and CMR Working Group of the European Society of Cardiology consensus statement. *J Cardiovasc Magn Reson* 15(1):92–92
  23. Robbers LF, Baars EN, Brouwer WP, Beek AM, Hofman MB, Niessen HW, van Rossum AC, Marcu CB (2012) T1 mapping shows increased extracellular matrix size in the myocardium due to amyloid depositions. *Circ Cardiovasc Imaging* 5(3):423–426
  24. Soler R, Rodriguez E, Remuinan C, Bello MJ, Diaz A (2003) Magnetic resonance imaging of primary cardiomyopathies. *J Comput Assist Tomogr* 27(5):724–734